

# The Effect of DIC Parameters in the Measurement of Stress Intensity Factors $K_I$ and $K_{II}$

Lenny Iryani\*, Tatacipta Dirgantara<sup>1</sup>,  
Sandro Mihradi, Ichsan Setya Putra

Faculty of Mechanical and Aerospace Engineering  
Institut Teknologi Bandung  
Ganesha 10, Bandung 40132, INDONESIA

<sup>1</sup>Corresponding Author: [tdirgantara@ftmd.itb.ac.id](mailto:tdirgantara@ftmd.itb.ac.id)

## ABSTRACT

*In the present work, the effect of several Digital Image Correlation (DIC) parameters to the accuracy of the Stress Intensity Factors ( $K$ ), was investigated. The values of  $K_I$  and  $K_{II}$  were estimated in a three point bend specimen from the displacement field values around the crack tip obtained experimentally by using the DIC technique, using non-linear least square technique together with Taylor's expansion. It was found that some DIC parameters i.e. subset and template area should be carefully chosen in order to obtain an accurate result. The results showed that by setting the subset and the template edge length ratio to be 0.2 – 0.6, the  $K$  of mode I and mode II were in good agreements compared to the finite element results. The maximum difference of  $K_I$  is 1.9% and  $K_{II}$  is 4.6%.*

**Keywords:** Digital Image Correlation, Stress Intensity Factor, Mode I, Mode II, Three Point Bend Experiment.

## Introduction

A good understanding of fracture-mechanics phenomena has contributed to a safer and more reliable structural design. In the application of fracture-mechanics concept to structural design and analysis, some primary parameters that affect the structural integrity with the presence of cracks has to be identified and quantified. One of the most widely used parameter is the Stress Intensity Factors (SIFs),  $K$ . This parameter is often used for describing the severity of the stresses in the vicinity of the crack tip, especially for linear elastic fracture mechanics analysis. For simple geometry the value of  $K$  can be found in the literature, see e.g. Rooke & Cartwright [1] or Murakami [2]. For more complex configurations, numerical methods such as finite element method (FEM) or boundary element method (BEM) are usually employed [3]. Experimentally, the SIFs can be determined by using Strain Gage ( $K$ -Gage or  $T$ -gage) [4,5]. Recently, by the advanced of digital technology, the  $K$  can be determined from the displacement field around crack tip obtained using Digital Image Correlation (DIC) technique, as reported in [6-10].

The DIC technique has been increasingly popular recently in experimental mechanics because it is relatively easy to use. It can provide accurate results with relatively simple and low cost equipment. The early DIC techniques was developed by Sutton *et al* [11,12], and has been applied

---

\*) on leave from Teknik Aeronautika Politeknik Negeri Bandung, Indonesia

for fracture mechanics problem [6-10]. In [8,10] the method was applied for mixed mode problem; however so far there is no information about the effect of DIC parameters to the accuracy of the result.

The present study focuses on the effect of some DIC parameters, i.e. spacing size, and the ratio of subset and template area to the accuracy of  $K_I$  and  $K_{II}$ . A three point bending specimen made of an acrylic polymer was used in this experiment. To obtain  $K_I$  and  $K_{II}$ , a slant crack was introduced. Displacement field in the vicinity of crack tip was measured using DIC technique and the  $K$  values were then estimated from the crack tip displacement field using non-linear least square technique and Taylor's expansion using several sets of DIC parameters. The results were then compared with  $K$  values obtained by finite element analysis using modified virtual crack closure technique.

## Digital Image Correlation

The basic concept of the DIC technique is to find “similarities” of two given images of an object (see Figure 1). The technique to calculate the “similarities” is relies on the existence of a distinct gray-scale which is digitized as pixel. The smallest square area in Figure 1 is one pixel. The “similarities” of the first image and the second image are calculated by correlating the gray scale intensity value in the first image with the gray scale intensity value in the second image as shown in Figure 1. The image in Figure 1(a) are then converted to the value of gray scale intensity as shown in Figure 1(b). The scale for the black is 0 and for the white is 255.

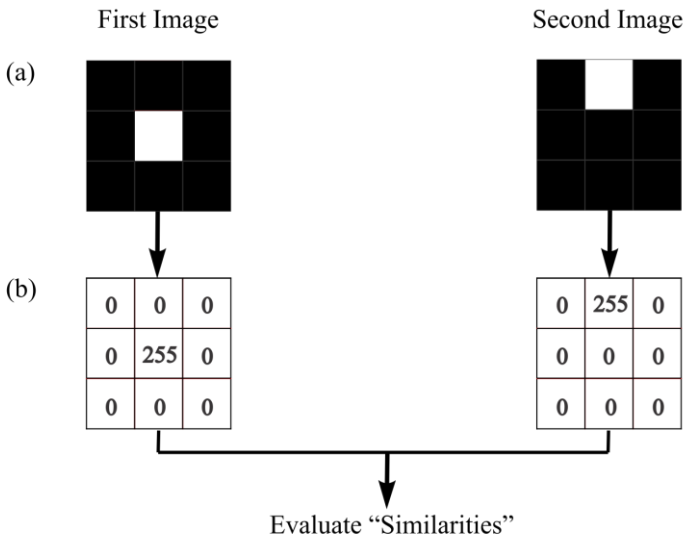


Figure 1: Evaluation process to find the similarity of the two images

Several correlation functions can be used to evaluate the similarity of the two images as described in [14]. According to Pan [14], the Zero-Normalized Cross Correlation (ZNCC) and Zero-Normalized Sum of Squared Differences (ZNSSD) correlation criterion offers the most robust noise-proof performance and is insensitive to the offset and linear scale in illumination lighting. In the present work, the ZNCC (Optimized Normalized Cross Correlation) function is chosen to be implemented in the developed DIC code.

The correlation function can be written as follow [13]:

$$C(i,j) = \frac{\sum_{m=0}^{M_{a-1}} \sum_{n=0}^{N_{a-1}} A(m,n) \cdot \text{conj} B(m+i,n+j)}{\sqrt{\sum_{m,n} A^2(m,n) \sum_{m,n} B^2(m+i,n+j)}} \quad (1)$$

where  $C$  is the normalized cross correlation value,  $A(m,n)$  is the pixel's gray-scale value of the subset located at row  $m$  and column  $n$  in the undeformed image, and  $B(m+i,n+j)$  is the pixel's gray-scale value of the sampling area located at row  $m+i$  and column  $n+j$  in the deformed image. Notations  $i$  and  $j$  correspond to the relative position of the center of the sampling area in the deformed image to the center of the subset in the undeformed image.

Figure 2 illustrates the process to measure the displacement at a certain point. The first step is to choose an area to be investigated in both the deformed and undeformed images. Both areas must have the same size and also the same center. The next step is to define a subset, which is a smaller area at the center of the previously chosen area in the undeformed image. The investigated area in the deformed image is called as template. The correlation of the subset to the template was then calculated by moving the subset pixel by pixel on the template. A matrix describing the values of correlation as a function of position in the template can be assembled as shown in Figure 2(b). The distance to move a template from the first position to the next position is defined as spacing. The displacement vectors were determined from the center of the subset in the reference image to the location of maximum correlation result in the template.

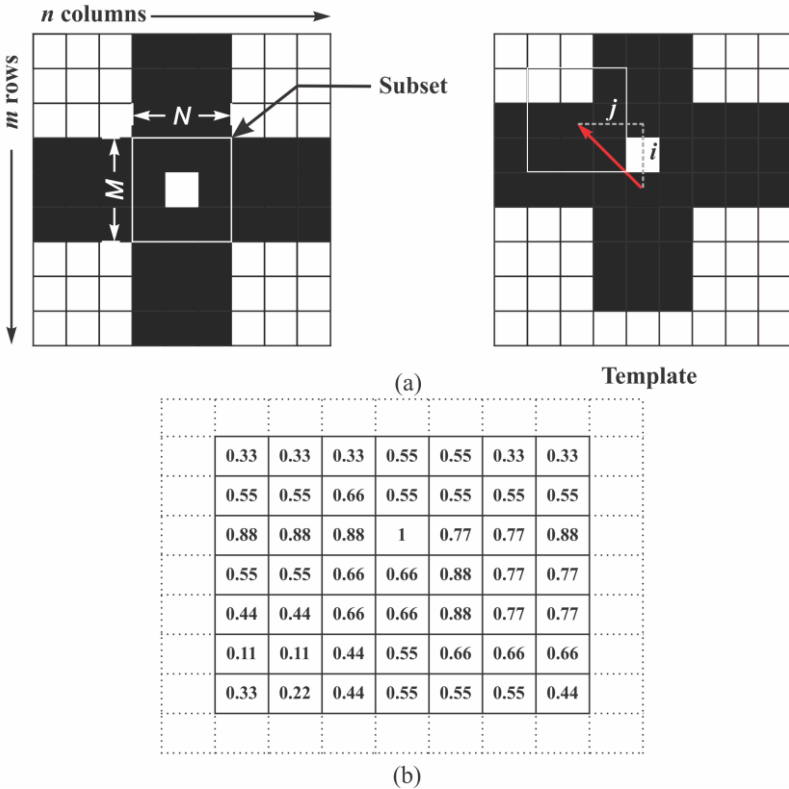


Figure 2: Schematic Process, (a) correlation process (b) matrix of degree of similarity

## Stress Intensity Factors Estimation

The analysis of the stress intensity factor in the present work was conducted for linear elastic fracture mechanics problem. Here, the value of *SIFs* for mixed mode cases are estimated from displacement field data obtained from DIC. The displacement fields around a crack tip for mode I and mode II loading with the rigid body movement correction can be expressed as [15].

$$\begin{aligned} \begin{Bmatrix} u_k \\ v_k \end{Bmatrix} = & \left( \sum_{n=1}^N \frac{A_{In}}{2G} r_k^{n/2} \begin{Bmatrix} \kappa \cos \frac{n}{2} \theta_k - \frac{n}{2} \cos \left( \frac{n}{2} - 2 \right) \theta_k + \left\{ \frac{n}{2} + (-1)^n \right\} \cos \frac{n}{2} \theta_k \\ \kappa \sin \frac{n}{2} \theta_k + \frac{n}{2} \sin \left( \frac{n}{2} - 2 \right) \theta_k - \left\{ \frac{n}{2} + (-1)^n \right\} \sin \frac{n}{2} \theta_k \end{Bmatrix} \right) \\ & - \left( \sum_{n=1}^N \frac{A_{II n}}{2G} r_k^{n/2} \begin{Bmatrix} \kappa \sin \frac{n}{2} \theta_k - \frac{n}{2} \sin \left( \frac{n}{2} - 2 \right) \theta_k + \left\{ \frac{n}{2} - (-1)^n \right\} \sin \frac{n}{2} \theta_k \\ -\kappa \cos \frac{n}{2} \theta_k - \frac{n}{2} \cos \left( \frac{n}{2} - 2 \right) \theta_k + \left\{ \frac{n}{2} - (-1)^n \right\} \cos \frac{n}{2} \theta_k \end{Bmatrix} \right) \\ & + \begin{pmatrix} T_x - Ry_k \\ T_y + Rx_k \end{pmatrix} \end{aligned} \quad (2)$$

where  $u_k$  and  $v_k$  are the displacement components in  $x$ -direction and  $y$ -direction at a point  $k$  respectively,  $G$  gives the shear modulus of the material,  $\kappa$  is  $(3 - \nu)/(1 + \nu)$  for plane stress and  $(3 - 4\nu)$  for plane strain,  $\nu$  is the Poisson's ratio and  $N$  is the number of terms of the series expansion of the displacement field. It may be noted that translation and rigid body rotation are represented in Eq. (2) by  $T$  and  $R$ .  $r_k$  and  $\theta_k$  is the position of point  $k$  from the crack tip, as shown in Figure 3.

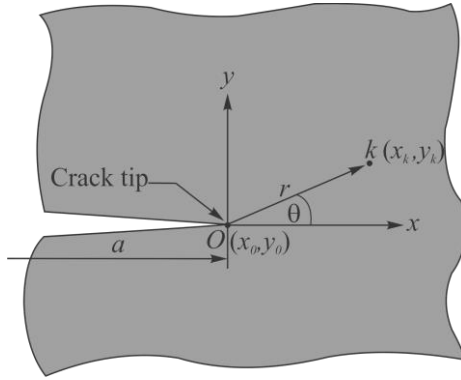


Figure 3: Coordinates System of point  $k$  from crack tip.

In polar coordinates, the position is defined as

$$r_k = \sqrt{(x_k - x_0)^2 + (y_k - y_0)^2} \quad ; \quad \theta_k = \tan^{-1} \left( \frac{y_k - y_0}{x_k - x_0} \right) \quad (3)$$

where  $x_0$  and  $y_0$  are the crack tip position relative to an arbitrary Cartesian coordinate system. An important parameter to determined  $K$  in Eq. (2) is  $A$ . The value of  $K_I$  and  $K_{II}$  can be obtained through the relation of  $A_I = K_I/\sqrt{2\pi}$  and  $A_{II} = -K_{II}/\sqrt{2\pi}$  respectively.

If the crack tip coordinate is known, Eq. (2) become linear equations with the unknown coefficients are:  $A_{In}$ ,  $A_{II n}$ ,  $T_x$ ,  $T_y$ , and  $R$ . Unfortunately, the crack tip position  $(x_0, y_0)$  could not be obtained directly from DIC technique because only the gray-scale intensity of the image is provided. Hence, the crack tip position should be treated as an unknown parameter as well, as in [8]. If all of the displacement values of numerous points from DIC result are

used, an over-determined set of simultaneous equations is obtained, and the problem could not be solved directly, and a nonlinear least-square technique using Newton-Raphson method is applied. Eq. (2) represent the nonlinear problem with the unknown parameters are  $A_{In}$ ,  $A_{IIn}$ ,  $T_x$ ,  $T_y$ ,  $R$ ,  $x_0$  and  $y_0$ . At the beginning of calculation process, the initial value of  $x_0$ ,  $y_0$  will be estimated, i.e. as an initial crack tip.

The basic concept of least square technique is to minimize the error between the estimated values of  $u_k$  and  $v_k$  from Eq. (2) with DIC results, as shown in Eq. (4).

$$\begin{aligned} h_{xk} &= \sum_{n=1}^N \frac{A_{In}}{2G} r_k^{n/2} f_{In}(\theta_k) - \sum_{n=1}^N \frac{A_{IIn}}{2G} r_k^{n/2} f_{IIn}(\theta_k) + T_x - R y_k - u_k \\ h_{yk} &= \sum_{n=1}^N \frac{A_{In}}{2G} r_k^{n/2} f_{In}(\theta_k) - \sum_{n=1}^N \frac{A_{IIn}}{2G} r_k^{n/2} f_{IIn}(\theta_k) + T_y + R x_k - v_k \end{aligned} \quad (4)$$

where  $h_k$  is the error in the least square technique, and  $u_k$  and  $v_k$  are the displacement field data from DIC. Based on Taylor's series expansions, a series of iterative equations of Eq. (4) yields the following equations:

$$\begin{aligned} (h_{xk})_{i+1} &= (h_{xk})_i + \sum_{n=1}^N \left( \frac{\partial h_{xk}}{\partial A_{In}} \right)_i \Delta A_{In} + \sum_{n=1}^N \left( \frac{\partial h_{xk}}{\partial A_{IIn}} \right)_i \Delta A_{IIn} + \left( \frac{\partial h_{xk}}{\partial T_x} \right)_i \Delta T_x + \left( \frac{\partial h_{xk}}{\partial T_y} \right)_i \Delta T_y \\ &\quad + \left( \frac{\partial h_{xk}}{\partial R} \right)_i \Delta R + \left( \frac{\partial h_{xk}}{\partial x_0} \right)_i \Delta x_0 + \left( \frac{\partial h_{xk}}{\partial y_0} \right)_i \Delta y_0. \\ (h_{yk})_{i+1} &= (h_{yk})_i + \sum_{n=1}^N \left( \frac{\partial h_{yk}}{\partial A_{In}} \right)_i \Delta A_{In} + \sum_{n=1}^N \left( \frac{\partial h_{yk}}{\partial A_{IIn}} \right)_i \Delta A_{IIn} + \left( \frac{\partial h_{yk}}{\partial T_x} \right)_i \Delta T_x + \left( \frac{\partial h_{yk}}{\partial T_y} \right)_i \Delta T_y \\ &\quad + \left( \frac{\partial h_{yk}}{\partial R} \right)_i \Delta R + \left( \frac{\partial h_{yk}}{\partial x_0} \right)_i \Delta x_0 + \left( \frac{\partial h_{yk}}{\partial y_0} \right)_i \Delta y_0. \end{aligned} \quad (5)$$

where subscript  $i$  denotes the  $i$ th iteration step, and  $\Delta A_{In}$ ,  $\Delta A_{IIn}$ ,  $\Delta T_x$ ,  $\Delta T_y$ ,  $\Delta R$ ,  $\Delta x_0$  and  $\Delta y_0$  are corrections to the previous estimation of  $A_{In}$ ,  $A_{IIn}$ ,  $T_x$ ,  $T_y$ ,  $R$ ,  $x_0$  and  $y_0$ . The value of  $(h_{xk})_{i+1}$  and  $(h_{yk})_{i+1}$  should be approaching zero on the last iteration step. Assuming that  $(h_{xk})_{i+1}$  and  $(h_{yk})_{i+1}$  is equal to zero, Eq. (5) can be written as follow:

$$\begin{aligned} -(h_{xk})_i &= \sum_{n=1}^N \left( \frac{\partial h_{xk}}{\partial A_{In}} \right)_i \Delta A_{In} + \sum_{n=1}^N \left( \frac{\partial h_{xk}}{\partial A_{IIn}} \right)_i \Delta A_{IIn} + \left( \frac{\partial h_{xk}}{\partial T_x} \right)_i \Delta T_x + \left( \frac{\partial h_{xk}}{\partial T_y} \right)_i \Delta T_y \\ &\quad + \left( \frac{\partial h_{xk}}{\partial R} \right)_i \Delta R + \left( \frac{\partial h_{xk}}{\partial x_0} \right)_i \Delta x_0 + \left( \frac{\partial h_{xk}}{\partial y_0} \right)_i \Delta y_0. \\ -(h_{yk})_i &= \sum_{n=1}^N \left( \frac{\partial h_{yk}}{\partial A_{In}} \right)_i \Delta A_{In} + \sum_{n=1}^N \left( \frac{\partial h_{yk}}{\partial A_{IIn}} \right)_i \Delta A_{IIn} + \left( \frac{\partial h_{yk}}{\partial T_x} \right)_i \Delta T_x + \left( \frac{\partial h_{yk}}{\partial T_y} \right)_i \Delta T_y \\ &\quad + \left( \frac{\partial h_{yk}}{\partial R} \right)_i \Delta R + \left( \frac{\partial h_{yk}}{\partial x_0} \right)_i \Delta x_0 + \left( \frac{\partial h_{yk}}{\partial y_0} \right)_i \Delta y_0. \end{aligned} \quad (6)$$

Equation (6) can be written in matrix form as

$$[h] = [d][\Delta] \quad (7)$$

where

$$[h] = \begin{bmatrix} -h_{xI} \\ \vdots \\ -h_{xM} \\ -h_{yI} \\ \vdots \\ -h_{yM} \end{bmatrix}; \quad [d] = \begin{bmatrix} \frac{\partial h_{xI}}{\partial A_{I1}} & \dots & \frac{\partial h_{xI}}{\partial A_{II1}} & \dots & \frac{\partial h_{xI}}{\partial T_x} & 0 & \frac{\partial h_{xI}}{\partial R} & \frac{\partial h_{xI}}{\partial x_o} & \frac{\partial h_{xI}}{\partial y_o} \\ \vdots & \ddots & \vdots & \vdots & \vdots & \vdots & \vdots & \vdots & \vdots \\ \frac{\partial h_{xM}}{\partial A_{I1}} & \dots & \frac{\partial h_{xM}}{\partial A_{II1}} & \dots & \frac{\partial h_{xM}}{\partial T_x} & 0 & \frac{\partial h_{xM}}{\partial R} & \frac{\partial h_{xM}}{\partial x_o} & \frac{\partial h_{xM}}{\partial y_o} \\ \frac{\partial h_{yI}}{\partial A_{I1}} & \dots & \frac{\partial h_{yI}}{\partial A_{II1}} & \dots & 0 & \frac{\partial h_{yI}}{\partial T_y} & \frac{\partial h_{yI}}{\partial R} & \frac{\partial h_{yI}}{\partial x_o} & \frac{\partial h_{yI}}{\partial y_o} \\ \vdots & \ddots & \vdots & \vdots & \vdots & \vdots & \vdots & \vdots & \vdots \\ \frac{\partial h_{yM}}{\partial A_{I1}} & \dots & \frac{\partial h_{yM}}{\partial A_{II1}} & \dots & 0 & \frac{\partial h_{yM}}{\partial T_y} & \frac{\partial h_{yM}}{\partial R} & \frac{\partial h_{yM}}{\partial x_o} & \frac{\partial h_{yM}}{\partial y_o} \end{bmatrix};$$

$$[\Delta] = \begin{bmatrix} \Delta A_{I1} \\ \vdots \\ \Delta A_{II1} \\ \vdots \\ \Delta T_x \\ \Delta T_y \\ \Delta R \\ \Delta x_o \\ \Delta y_o \end{bmatrix} \quad (8)$$

$M$  in Eq. (8) is the total number of displacement data. Using the least squares technique, the value  $\Delta$  in Eq. (7) in one step iteration is given by

$$\Delta = \left[ [d]^T [d] \right]^{-1} [d]^T [h] \quad (9)$$

The value of  $\Delta$  gives the correction terms for prior estimates of the coefficients of the unknown parameters as given in Eq. (10).

$$\begin{aligned} (A_{In})_{i+1} &= (A_{In})_i + \Delta A_{In} \\ (A_{II n})_{i+1} &= (A_{II n})_i + \Delta A_{II n} \\ (T_x)_{i+1} &= (T_x)_i + \Delta T_x \\ (T_y)_{i+1} &= (T_y)_i + \Delta T_y \\ (R)_{i+1} &= (R)_i + \Delta R \\ (x_o)_{i+1} &= (x_o)_i + \Delta x_o \\ (y_o)_{i+1} &= (y_o)_i + \Delta y_o \end{aligned} \quad (10)$$

The iterative procedure is repeated until the corrections become acceptably small and finally the unknown parameters will be obtained. The flow chart of the algorithm to obtain the value of  $K_I$  and  $K_{II}$  are shown in Figure 4. In this work, the algorithm was developed by using MATLAB R2009 software.

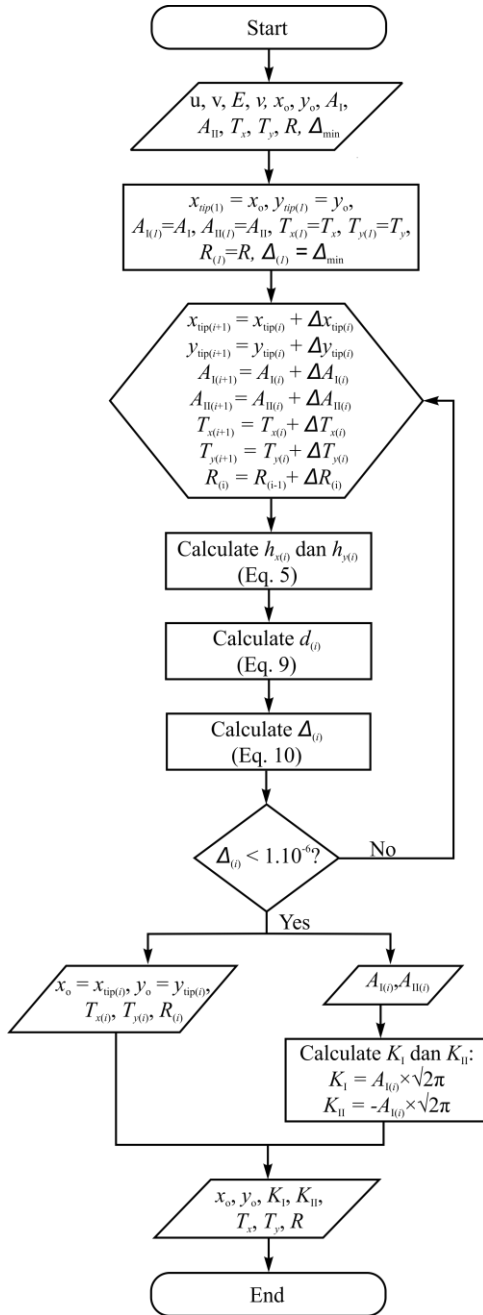


Figure 4. Flowchart of the algorithm to obtain  $K_I$  and  $K_{II}$

## Experiment

### Specimens and Material

The experiments to obtain  $K_I$  and  $K_{II}$  were performed on a three point bend specimen. The geometry of the specimen is shown in Figure 5 with  $a = 20$  mm,  $W = 50$  mm and  $t = 6$  mm. A slant crack with an angle  $45^\circ$  was introduced with laser cutting on one side of the specimen. The width of the crack is 0.15 mm. The material used in these experiments was cast acrylic sheet with modulus of elasticity,  $E = 2.896$  GPa and the Poisson's ratio = 0.402.

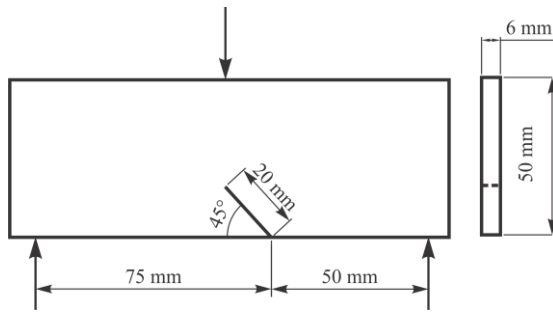


Figure 5: Geometry of the three point bend specimen

To provide the specimen's surface with a certain gray-scale intensity for the displacement measurement, random speckle patterns was introduced by black and white spray paint, as can be seen in Figure 6. Black spray paint was sprayed first, as the base paint. The white paint creates white dots over the base paint. In general the average of the radius of white dots is 4 pixel.

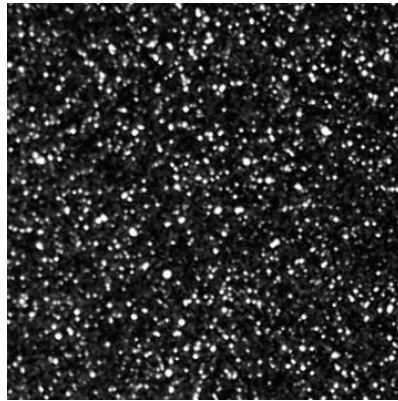


Figure 6: Random Speckle Pattern ( $358 \times 358$  pixel<sup>2</sup>)

### Experimental Procedure

The equipment used in this experiment are a Personal Computer (PC), a Universal Testing Machine Lloyd Instrument (Nexygen LRX Plus), a High Resolution Digital SLR Camera (Canon EOS 20D and 30D) and a white light source which is used to provide lights on the specimen's surface during the experiments. The personal computer was connected to the testing machine and controlled the machine's action. The capacity of the testing machine used in this experiment is 5 kN.

To convert the image size unit from pixel to the unit of length, a calibration process using a checkerboard pattern has to be conducted before the experiment. The camera should be placed perpendicular to the specimen, and the region of interest is placed at the center of the image, in order to minimize distortion.

The experimental set up of the equipment for three point bend experiment was shown in Figure 7. The camera's position is perpendicular to the specimen's surface and it's distance is about 300 mm.



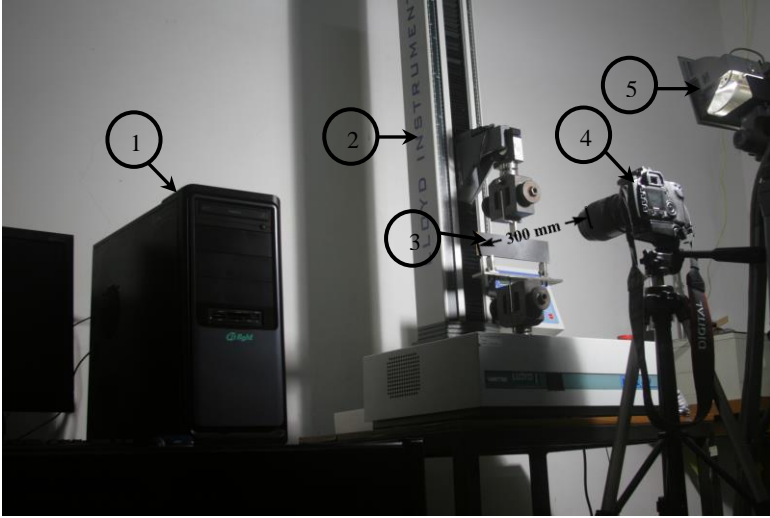


Figure 7. Set up of the three point bend experiment. 1: PC; 2: Universal Testing Machine; 3: Specimen; 4: Digital Camera; 5: White Light Source

Figure 8(a) shows the photograph of the specimen. The 300 mm image is then rotated so that the crack is parallel to the x-axis, as shown in figure 8(b). The region of interest around the crack tip for analysis is then chosen by cropping the image, as can be seen in figure 8(c).

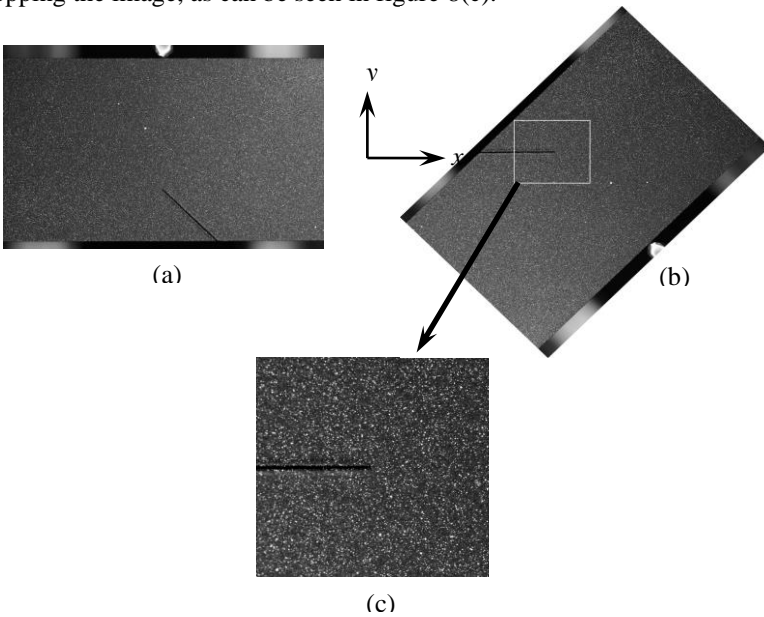


Figure 8: (a) Original Image, (b) Rotated Image (135°) and (c) Interrogation Area

## Results and Discussion

Using the DIC technique, the displacements of a large number of points in the vicinity of the crack tip can be obtained. The displacements are then used for iterative procedure presented in equations 2 – 6 to estimate the values of  $K_I$  and  $K_{II}$ . It should be noted that the present DIC technique to estimate the value of  $K_I$  and  $K_{II}$  is valid for all materials, as long as the case can still be considered to be a Linear Elastic Fracture Mechanics Problem. To investigate the effect of the DIC parameters to the accuracy of  $K_I$  and  $K_{II}$ , in this work,

several spacing sizes, and several ratios between subset and tempale edge length are exploited to obtain  $K$  values. The results were then compared with the finite element results [16]. Two level of loading were employed, i.e. 200 N and 250 N. The load was chosen as such to ensure that the displacement vectors can be observed properly using DIC technique.

### Effect of the Spacing Size

To see the effect of the spacing size to the accuracy of  $K_I$  and  $K_{II}$ , a constant load  $P = 200$  N was used. The spacing sizes used in this analysis was 20, 30, 40 and 50 pixel. Before analyzing the effect of spacing size,  $K_I$  and  $K_{II}$  were plotted as a function of the number of terms of the displacement field series expansion  $N$  using the spacing size 30 pixel. Figure 9 shows the normalized  $K_I$  and  $K_{II}$ , where  $K_0 = (15P\sqrt{\pi a})/(4tW)$ . It can be seen that after  $N = 6$ , the value of  $K_I$  and  $K_{II}$  were already converge. In this present study, the value of  $K_I$  and  $K_{II}$  were taken at  $N = 10$ .

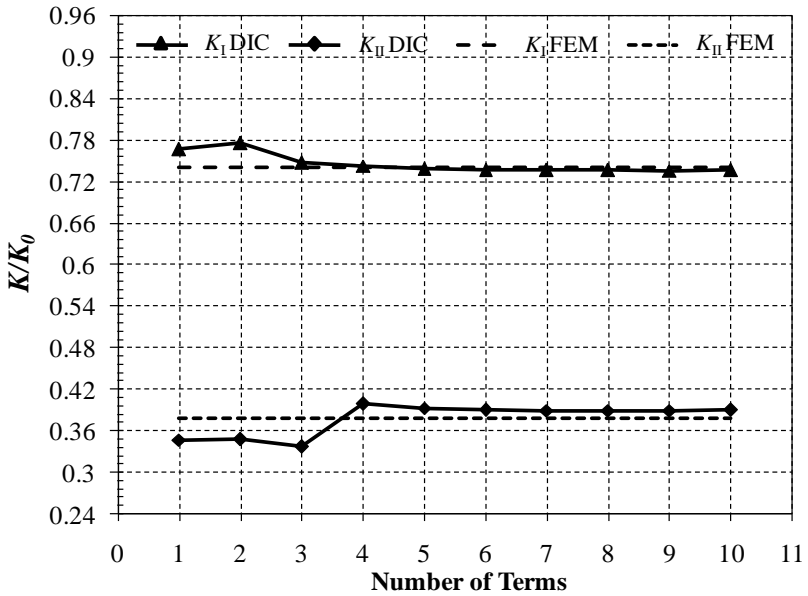


Figure 9: Effect Number of Terms,  $N$  to the  $K_I$  and  $K_{II}$

Figure 10 shows the values of normalized  $K_I$  and  $K_{II}$  plotted as a function of spacing size. It can be seen that the normalized values of  $K_I$  and  $K_{II}$  on spacing size 20, 30, 40, and 50 pixel are in good agreements with the finite element results [16], with about 3% maximum difference. From this result it can be concluded that within the observed spacing sizes, the spacing size does not significantly affect the value of  $K_I$  and  $K_{II}$ .

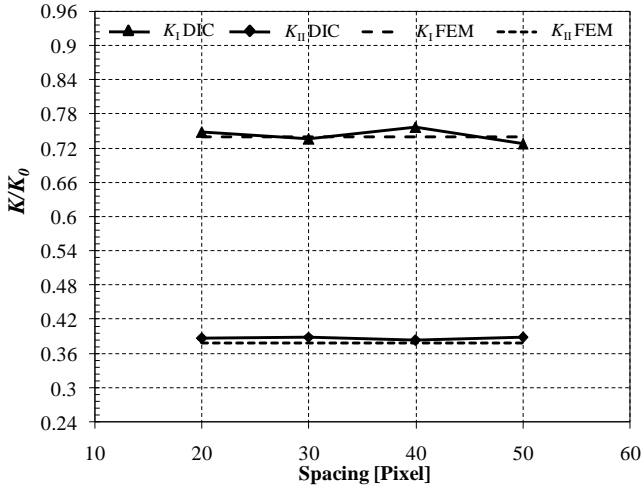


Figure 10:  $K_I$  and  $K_{II}$  for four different spacing size

### Effect of the Ratio between the Subset and the Template Edge Length

In this analysis, the ratio of the subset and the template edge length,  $\ell$ , were set to be 0.2 – 0.8, and the template edge length is 100 pixel. The results can be seen in Figure 11.

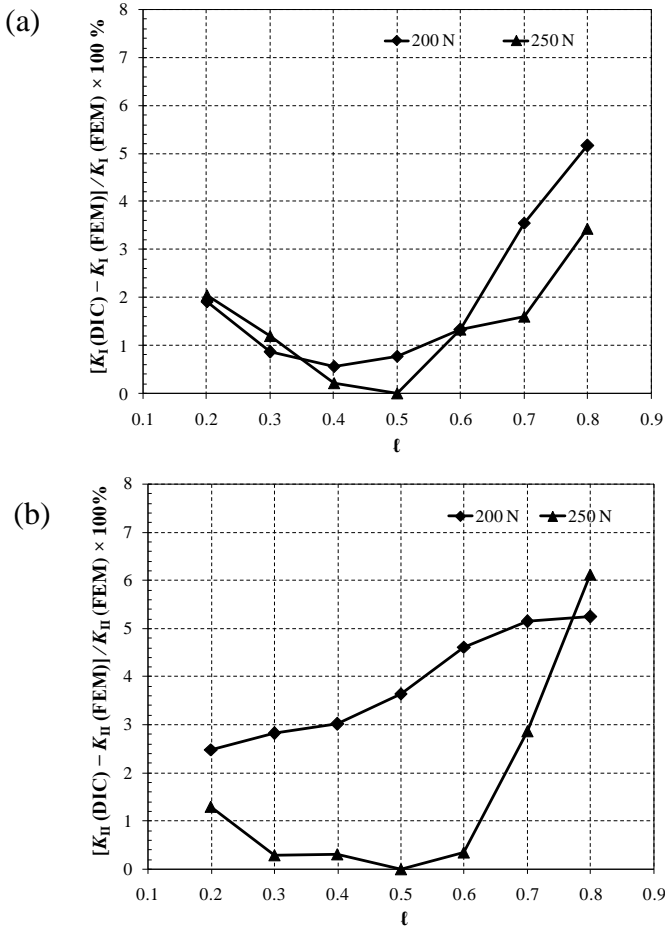


Figure 11: Error of  $K_I$  and  $K_{II}$  for the set of the ratio of subset and template edge size,  $\ell$

From Figure 11(a) it can be seen that the difference of  $K_I$  obtained by DIC compared to the finite element result [16] is less than 3% for the ratio of subset and template edge size 0.2 – 0.6. Meanwhile in Figure 11(b) the difference of  $K_{II}$  for the ratio of subset and template edge size 0.2 – 0.6 is less than 5% compared to the finite element result [16]. It can be seen that in order to achieve maximum differences of  $K_I$  and  $K_{II}$  less than 5%, it is recommended to use the ratio of subset and template edge size 0.2 – 0.6.

## Conclusions

In this work, the effect of DIC parameters, i.e. spacing size and the ratio of the subset and the template edge size, to the accuracy of mode I and mode II stress intensity factors estimated from DIC displacement field data has been presented. It can be concluded that within the observed sizes, the spacing size did not affect the accuracy of  $K_I$  and  $K_{II}$  but the proper choice of the subset to template edge length ratio can contribute to the accuracy of  $K$ . The present study showed that the ratio between 0.2 to 0.6 provide a good agreement with finite element result, with maximum differences are about 1.9% and 4.6% for  $K_I$  and  $K_{II}$  respectively.

## Acknowledgement

This work was carried out with the financial support from “Penguatan Riset Institusi (PRI) ITB 2010” and “Riset KK ITB 2011”.

## References

- [1] D.P. Rooke, D.J. Cartwright: “Compendium of Stress Intensity Factors”, 1<sup>st</sup> edition, The Hillingdon Press (1974).
- [2] Murakami. Y: “Stress Intensity Factors Handbook”, Vol.2, Pergamon Books Ltd. (1987).
- [3] Milne, I, Ritchie, R.O., Karihaloo, B: “Comprehensive Structural Integrity”, Vol. 3, Numerical and Computational Method, Elsevier (2003).
- [4] I.S. Putra: “Some experience in using the K-gage to measure stress intensity factors”, Proceedings of Damage and Fracture Mechanics, Montreal, Canada (2000).
- [5] M.J. Maleski, M.S. Kirugulige and H.V. Tippur, “A Method For Measuring Mode I Crack Tip Constraint Under Static And Dynamic Loading Conditions”, Society for Experimental Mechanics, Vol. 44, No. 5 (October 2004).
- [6] S. Yoneyama, Y. Morimoto, and M. Takashi, ”Automatic Determination Method of Stress Intensity Factor Utilizing Digital Image Correlation and Nonlinear Least Square”, Structural Health Monitoring and Intelligent Infrastructure, p. 1379 (2003).
- [7] S. Roux, F. Hild, “Stress intensity factor measurements from digital image correlation: post-processing and integrated approaches”, Int. J. Fract., 140, p. 141-157 (2006).
- [8] S. Yoneyama, T. Ogawa, and Y. Kobayashi, “Evaluating Mixed-Mode Stress Intensity Factors from Full-Field Displacement Fields Obtained by Optical Methods”. Engineering Fracture Mechanics, p. 1399-1412 (2007).
- [9] J. Réthoré, S. Roux, F. Hild, “An extended and integrated digital image correlation technique applied to the analysis fractured samples”, Eur. J. Comput. Mech., p. 285-30618 (2009).

- [10] Zhang R, He L. "Measurement of mixed-mode stress intensity factors using digital image correlation method", *Optics and Lasers in Engineering* 50, p. 1001–1007 (2012).
- [11] M. A. Sutton, W. J. Wolters, W. H. Peters, W. F. Ranson, and S. R. Mc. Neill: "Determination of Displacement Using an Improved Digital Image Correlation Method", *Image Vis. Comput.*, 1:133 (1983).
- [12] M. A. Sutton, M. Cheng, S. R. Mc. Neill, Y. J. Chao, and W. H. Peters: "Application of an Optimized on Digital Correlation Method to Planar Deformation Analysis", *Image Vis. Comput.*, 4:143 (1988).
- [13] T. Dirgantara, A. Sukmajaya, I.S. Putra, "Performance Evaluation of The Correlation and Smoothing Methods of The Digital Image Correlation and Its Application to The Opening Specimens", *Fourth International Conference on Experimental Mechanics, Singapore, Proceeding SPIE, Vol. 7522, 75224J*, editor: C. Quan, K. Qian, Anand K. Asundi, F. S. Chau (2010).
- [14] Bing Pan, Kemaq Qian, Huimin Xie and Anand Asundi, "Two-dimensional digital image correlation for in-plane displacement and strain measurement: a review", *Meas. Sci. Technol.* 20 062001, 1 - 17 (2009).
- [15] Kobayashi, Albert S, "Handbook on Experimental Mechanics", Prentice-Hall, Inc., 893 (1987).
- [16] I. Sutowo, D. Widagdo, T. Dirgantara, I. S. Putra, "Perhitungan Numerik Faktor Intensitas Tegangan Modus III menggunakan Teknik Pengatupan Retak Maya", *Prosiding Seminar Nasional Teknik Mesin X*, Nov, Malang (2011).